The rise of the primordial tensor spectrum from an early scalar-tensor epoch

Debika Chowdhury

Department of Physics, Swansea University

This talk is based on: *D. Chowdhury, G. Tasinato, and I. Zavala, JCAP* **08**, *010 (2022) (arXiv:2204.10218 [gr-qc])*.

August 20, 2022

Outline of the talk

Timeline of the universe[1]

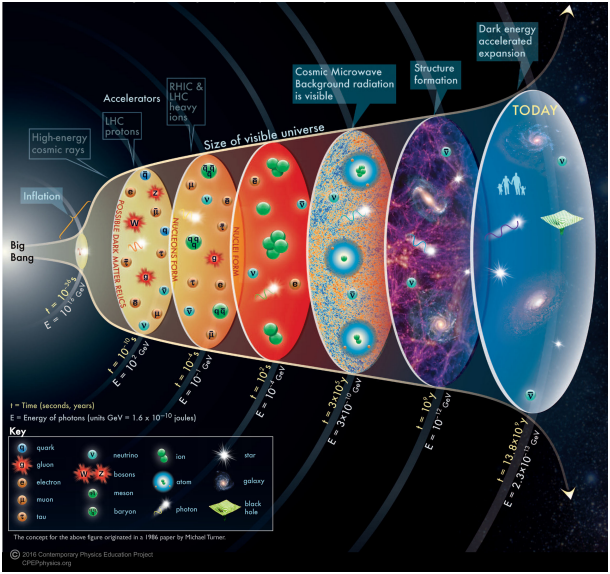

[1] Image from https://www.cpepphysics.org/images/expansion.jpg.

The unconstrained window of time

The standard ΛCDM model+inflation has been very successful in accounting for the most recent cosmological observations. Our current concept about the universe's evolution after BBN is backed by observations.

It leaves a window of time, from after the end of inflation to BBN, which is not yet well constrained.

As long as the expansion rate matches the standard (GR) value before the onset of BBN, the modifications due to non-trivial dynamics would not cause disagreements with the observations.

The modification of the expansion rate would leave imprints on the primordial gravitational waves generated over a particular range of frequencies, which can possibly be detected by future gravitational wave measurements.

PGW spectrum in standard cosmology I

Equation of motion for primordial tensor fluctuations[2]:

$$\ddot{h}_{ij} + 3H\dot{h}_{ij} - \frac{\nabla^2}{a^2} h_{ij} = 0.$$

To solve the tensor perturbation equations, one can write it in Fourier space as

$$h_{ij}(t, \vec{x}) = \sum_{\lambda} \int \frac{d^3k}{(2\pi)^3} h^{\lambda}(t, \vec{k}) \epsilon^{\lambda}_{ij}(\vec{k}) e^{i\vec{k}\cdot\vec{x}}.$$

Energy density of the relic GW:

$$\rho_{\rm GW}(t) = \frac{1}{16\pi G} \sum_{\lambda} \int \frac{d^3k}{(2\pi)^3} |\dot{h}^{\lambda}(t, \vec{k})|^2 .$$

Relic density of the PGWs:

$$\Omega_{\rm GW}(t, k) = \frac{1}{\rho_c(t)} \frac{d\rho_{\rm GW}(t, k)}{d \ln k}.$$

[2] Y. Watanabe and E. Komatsu, Phys. Rev. D **73**, 123515 (2006); K. Saikawa and S. Shirai, JCAP **05**, 035 (2018); N. Bernal and F. Hajkarim, Phys. Rev. D **100**, 063502 (2019); N. Bernal, *et al.*, JCAP **11**, 015 (2020).

PGW spectrum in standard cosmology II

Fractional energy density in primordial gravitational waves, observed today:

$$\boxed{\Omega^0_{\rm GW}(k)\,h^2 \simeq \frac{1}{24}\,\mathcal{P}_{\rm T}(k)\,\left(\frac{g_{*s,0}}{g_{*s,\rm hc}}\right)^{4/3}\,\left(\frac{T_0}{T_{\rm hc}}\right)^4\,\left(\frac{H_{\rm hc}}{H_0/h}\right)^2,}$$

where $\mathcal{P}_{\rm T} = r\,\mathcal{A}_{\rm S}$.

Frequency of GWs observed today:

$$\boxed{f_0 = 2.61745\times 10^{-8}\,\left(\frac{g_{*s,\rm hc}}{100}\right)^{-1/3}\,\left(\frac{g_{*,\rm hc}}{100}\right)^{1/2}\,\left(\frac{T_{\rm hc}}{1\,\rm GeV}\right)\ \rm Hz.}$$

Scalar-tensor theories

Action[3]:

$$S = S_{\rm EH} + S_\phi + S_m,$$

where

$$S_{\rm EH} = \frac{1}{2\kappa^2}\int {\rm d}^4x\,\sqrt{-g}\,R,$$

$$S_\phi = -\int {\rm d}^4x\,\sqrt{-g}\left[\frac{b}{2}(\partial\phi)^2 + M^4C^2(\phi)\sqrt{1+\frac{D(\phi)}{C(\phi)}\,(\partial\phi)^2} + V(\phi)\right],$$

$$S_m = -\int {\rm d}^4x\,\sqrt{-\tilde{g}}\,\mathcal{L}_M(\tilde{g}_{\mu\nu}),$$

with $\kappa^2 = M_{\rm Pl}^{-2} = 8\,\pi\,G$.

The disformally coupled metric is given by

$$\tilde{g}_{\mu\nu} = C(\phi)\,g_{\mu\nu} + D(\phi)\,\partial_\mu\phi\,\partial_\nu\phi.$$

[3] B. Dutta, E. Jimenez, and I. Zavala, JCAP **06**, 032 (2017); B. Dutta, E. Jimenez, and I. Zavala, Phys. Rev. D **96**, 103506 (2017).

Equations of motion

$$H^2 = \frac{\kappa^2}{3}\left[\rho_\phi + \rho\right],$$

$$\dot{H} + H^2 = -\frac{\kappa^2}{6}\left[\rho_\phi + 3P_\phi + \rho + 3P\right],$$

$$\ddot{\phi}\left[1 + \frac{b}{M^4 C D \gamma^3}\right] + 3H\dot{\phi}\,\gamma^{-2}\left[\frac{b}{M^4 C D \gamma} + 1\right]$$
$$+ \frac{C}{2D}\left(\gamma^{-2}\left[\frac{5C'}{C} - \frac{D'}{D}\right] + \frac{D'}{D} - \frac{C'}{C} - 4\gamma^{-3}\frac{C'}{C}\right) + \frac{1}{M^4 C D \gamma^3}\left(\mathcal{V}' + Q_0\right) = 0,$$

where

$$Q_0 = \rho\left[\frac{D}{C}\ddot{\phi} + \frac{D}{C}\dot{\phi}\left(3H + \frac{\dot{\rho}}{\rho}\right) + \left(\frac{D_{,\phi}}{2C} - \frac{D}{C}\frac{C_{,\phi}}{C}\right)\dot{\phi}^2 + \frac{C_{,\phi}}{2C}(1 - 3\omega)\right],$$

and

$$\rho_\phi = -\left[\frac{b}{2} + \frac{M^4 C D \gamma^2}{\gamma + 1}\right](\partial\phi)^2 + \mathcal{V}$$
$$P_\phi = -\left[\frac{b}{2} + \frac{M^4 C D \gamma}{\gamma + 1}\right](\partial\phi)^2 - \mathcal{V}.$$

Phenomenological scenario ($M = 0$, $b = 1$)

Causality constraint[4]: $C > 0$, $C + 2DX > 0$ with $X \equiv \frac{1}{2}(\partial\phi)^2$.

Master equation:

$$\frac{2\,(1+\lambda)}{3\,B}\,\varphi_{NN} + (2\,\lambda + 1 - w)\,\varphi_N + 2\,\lambda\,\frac{\mathrm{d}\ln V}{\mathrm{d}\varphi} + 2\left(1 - 3\,w\,\gamma^2\right)\alpha(\varphi)$$
$$+\frac{2\,\gamma^2\,(1+\lambda)}{3\,B}\,\frac{D\,\rho}{C}\left\{\varphi_{NN} - 3\,\varphi_N\left[w + \frac{\varphi_N^2}{6} + \frac{(1+w)\,B}{2\,(1+\lambda)}\right] + \frac{C}{2\,D}\left(\frac{D}{C}\right)_{,\varphi}\varphi_N^2\right\} = 0,$$

where

$$\gamma^{-2} = 1 - \frac{H^2}{\kappa^2}\,\frac{D}{C}\,\varphi_N^2.$$

Modified expansion rate:

$$\tilde{H}^2 = \frac{H^2\,\gamma^2}{C}\,[1 + \alpha(\varphi)\,\varphi_N]^2 = \frac{\kappa^2}{\kappa_{\mathrm{GR}}^2}\,\frac{\gamma^3\,C\,(1+\lambda)\,[1 + \alpha(\varphi)\,\varphi_N]^2}{B}\,H_{\mathrm{GR}}^2,$$

where

$$\kappa_{\mathrm{GR}}^2 = \kappa^2\,C(\varphi_0)\left[1 + \alpha^2(\varphi_0)\right], \qquad B = 1 - \frac{\varphi_N^2}{6}.$$

[4] J. D. Bekenstein, Phys. Rev. D **48**, 3641 (1993).

Purely conformal case ($D = 0$)

In this case, we have $\gamma = 1$.

The equation of motion simplifies to:

$$\frac{2}{3\left(1-\frac{\varphi_N^2}{6}\right)}\varphi_{NN} + (1-\tilde{w})\,\varphi_N + 2\,(1-3\,\tilde{w})\,\alpha(\varphi) = 0.$$

Change of variable:

$$\begin{aligned} N \equiv \ln\frac{a}{a_0} &= \ln\left[\frac{\tilde{T}_0}{\tilde{T}}\left(\frac{g_s(\tilde{T}_0)}{g_s(\tilde{T})}\right)^{1/3}\right] + \ln\left[\frac{C_0}{C(\varphi)}\right]^{1/2} \\ &= \ln\frac{\tilde{a}}{\tilde{a}_0} + \ln\left[\frac{C_0}{C(\varphi)}\right]^{1/2} \\ &= \tilde{N} + \ln\left[\frac{C_0}{C(\varphi)}\right]^{1/2}. \end{aligned}$$

The kick function

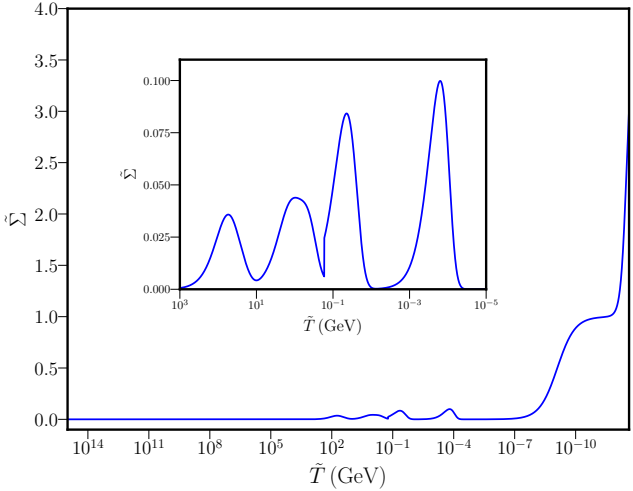

The behaviour of the 'kick function', $\tilde{\Sigma} = 1 - 3\,\tilde{w}$, has been plotted as a function of temperature.

Field evolution with zero initial velocity

We choose

$$C(\varphi) = (1 + b\,\mathrm{e}^{-\beta\varphi})^{2n},$$

with $b = 0.1,\ \beta = 8$.

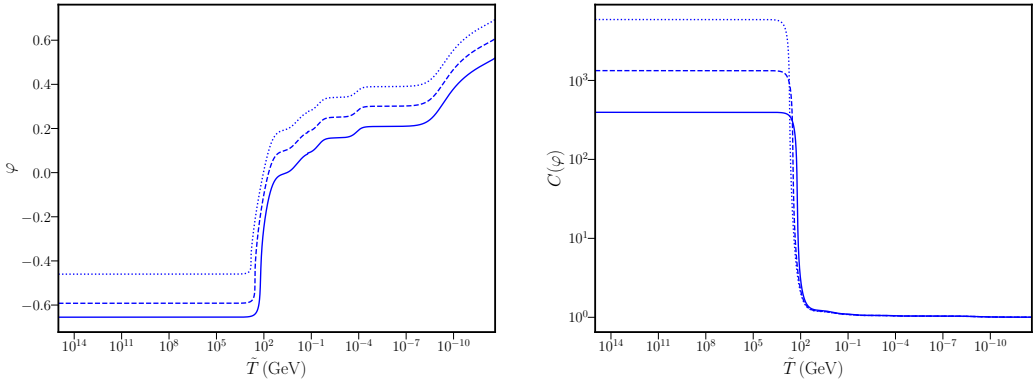

The evolution of the field and the conformal factor for $n = 1$ (solid blue line), $n = 2$ (dashed blue line), and $n = 4$ (dotted blue line).

Field evolution with negative initial velocity

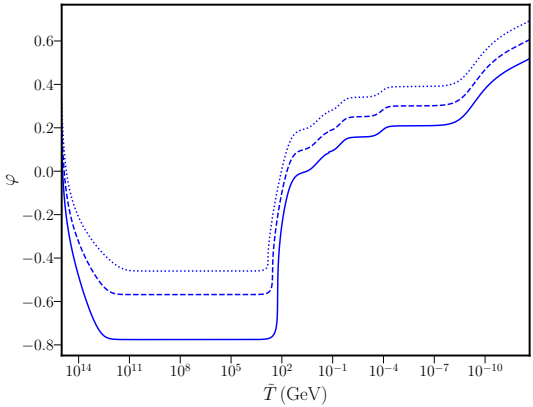

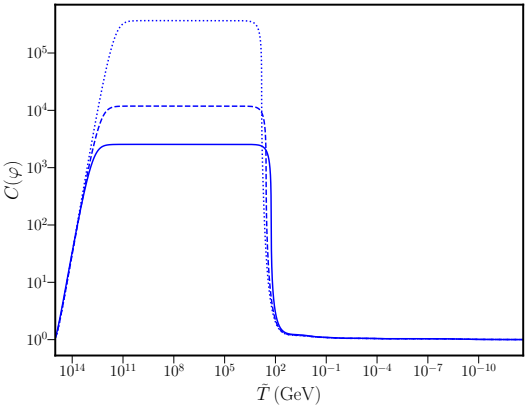

The evolution of the field and the conformal factor for $n = 1$ (solid blue line), $n = 2$ (dashed blue line), and $n = 4$ (dotted blue line), with the same conformal factor as in the previous plot.

Comparison of expansion rates

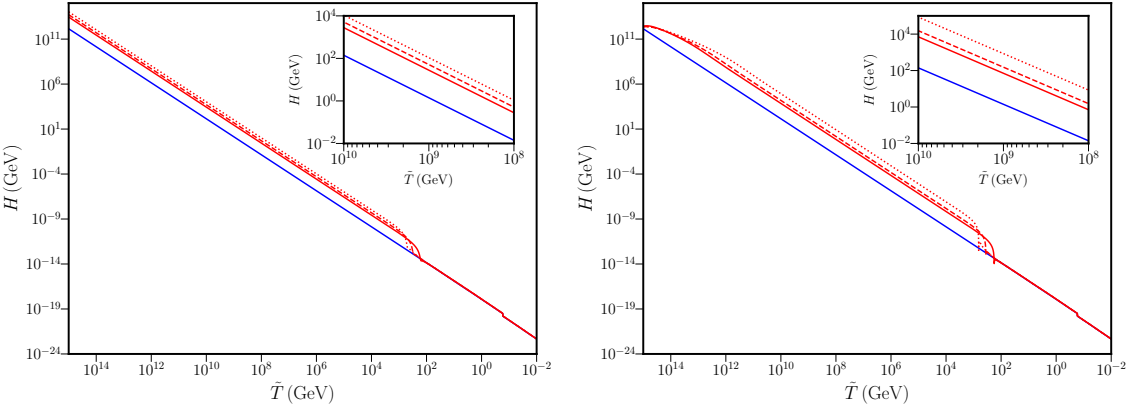

Comparison of expansion rates for the cases with zero initial velocity (on the left), and negative initial velocity (on the right). The Hubble parameter in the purely GR scenario has been plotted in blue, while the modified Hubble parameters have been plotted in red for $n = 1$ (solid red line), $n = 2$ (dashed red line), and $n = 4$ (dotted red line).

Comparison of GW spectra

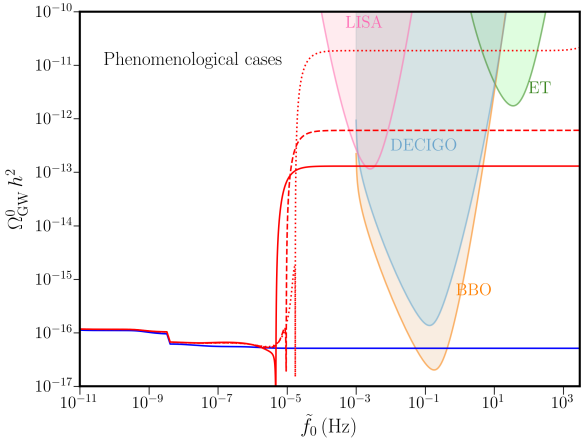

Comparison of GW spectra for the cases with $n = 1$ (solid red line), $n = 2$ (dashed red line), and $n = 4$ (dotted red line). The GW spectrum in the purely GR scenario has been plotted in blue.

Purely disformal case ($C = 1$)

Causality condition:

$$\left[D(\varphi)\, H^2\, \varphi_{\tilde{N}}^2/\kappa^2\right] - 1 < 0$$

Equations of motion:

$$H_{\tilde{N}} = -H\left[\frac{3\,B}{2}\left(1+\tilde{w}\gamma^{-2}\right) + \frac{\varphi_{\tilde{N}}^2}{2}\right],$$

$$\varphi_{\tilde{N}\tilde{N}}\left[1+\frac{3H^2\gamma^2 BD}{\kappa^2}\right] + \varphi_{\tilde{N}}\,\frac{H_{\tilde{N}}}{H}\left[1+\frac{3H^2\gamma^2 BD}{\kappa^2}\right] + 3\,\varphi_{\tilde{N}}\left[1-\frac{3H^2\tilde{w}BD}{\kappa^2}\right] + \frac{3H^2\gamma^2 BD}{\kappa^2}\,\delta(\varphi)\,\varphi_{\tilde{N}}^2 = 0,$$

where

$$B = 1 - \frac{\varphi_{\tilde{N}}^2}{6},$$

and

$$\gamma^{-2} = 1 - \frac{H^2}{\kappa^2}\,D(\varphi)\,\varphi_{\tilde{N}}^2.$$

Field evolution with constant and field dependent disformal factors

We choose $D = D_0$ and $D = D_0\,\varphi^2$.

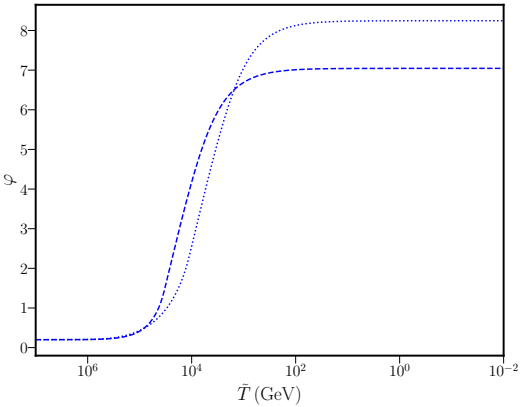

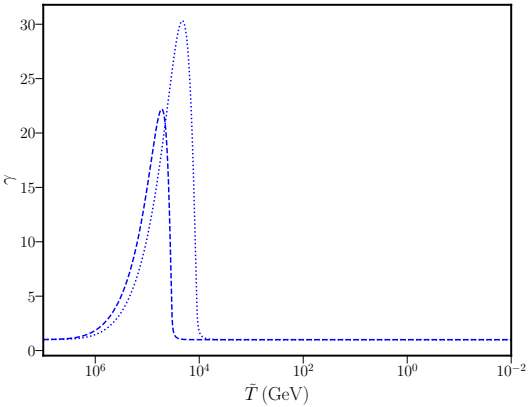

The evolution of the field and the Lorentz factor for $D = D_0$ (blue dashed lines) and $D = D_0\,\varphi^2$ (blue dotted lines).

Comparison of expansion rates

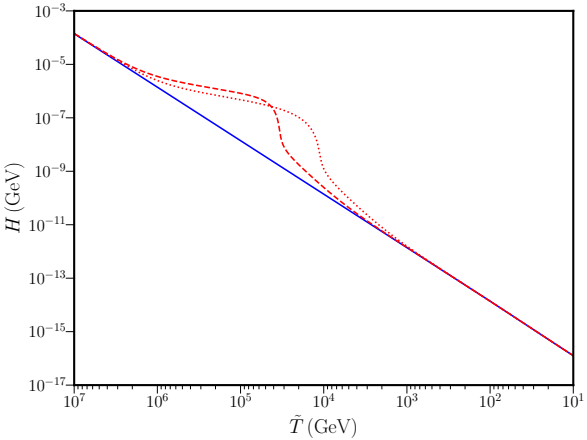

Comparison of expansion rates for the cases with constant disformal factor (red dashed line), and field dependent disformal factor (red dotted line). The Hubble parameter in the purely GR scenario has been plotted in blue.

Comparison of GW spectra

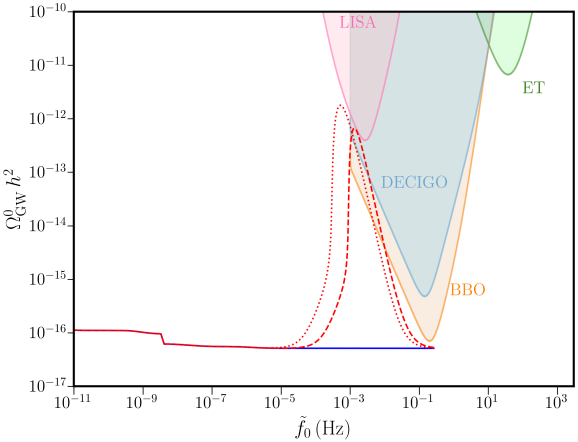

Comparison of GW spectra for the cases with constant disformal factor (red dashed line), and field dependent disformal factor (red dotted line). The GW spectra in the purely GR scenario has been plotted in blue.

Shifting the peaks of the GW spectra

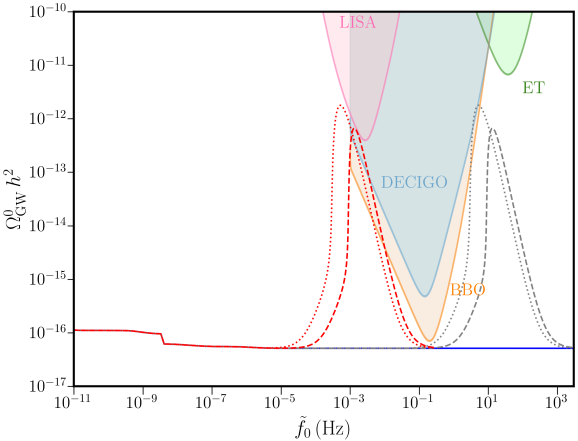

Comparison of GW spectra for the cases with constant disformal factor (red and grey dashed lines), and field dependent disformal factor (red and grey dotted lines). The GW spectra in the purely GR scenario has been plotted in blue.

D-brane scalar tensor scenario ($M \neq 0$, $b = 0$)

Normalization condition: $M^4 C D = 1$.

Equations of motion:

$$H = \frac{\kappa^2}{3}\frac{C^2\gamma}{B}\tilde{\rho}\,,$$

$$H_N = -H\left[\frac{3}{2}\left(1+\tilde{w}\,\gamma^{-2}\right)B + \frac{\varphi_N^2}{2}\,\gamma\right],$$

$$\varphi_{NN}\left[1+\frac{3\,H^2\,\gamma^{-1}\,B}{M^4\,C^2\,\kappa^2}\right] + 3\,\varphi_N\,\gamma^{-2}\left[1-\frac{3\,H^2\,\gamma^{-1}\,B}{M^4\,C^2\,\kappa^2}\,\tilde{w}\right] + \frac{H_N}{H}\,\varphi_N\left[1+\frac{3\,H^2\,\gamma^{-1}\,B}{M^4\,C^2\,\kappa^2}\right]$$
$$-\frac{6\,H^2\,\gamma^{-1}\,B}{M^4\,C^2\,\kappa^2}\,\alpha(\varphi)\,\varphi_N^2 + 3B\,\gamma^{-3}\alpha(\varphi)(1-3\,\tilde{w}) - \frac{2\,M^4\,C^2\,\kappa^2}{H^2}\left[2\,\gamma^{-3}-3\,\gamma^{-2}+1\right]\alpha(\varphi) = 0,$$

where

$$B = 1 - \frac{\gamma^2}{3(\gamma+1)}\varphi_N^2.$$

Purely disformal case ($C = 1$)

We have $D = 1/M^4$.

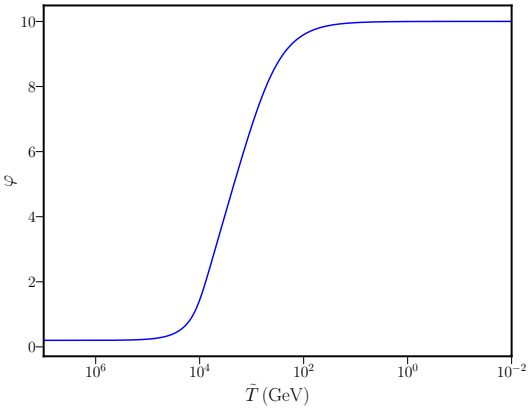

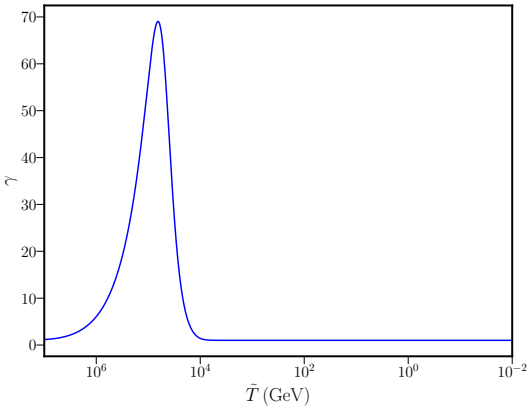

The evolution of the field and the Lorentz factor for the purely disformal scenario.

Expansion rate and GW spectrum

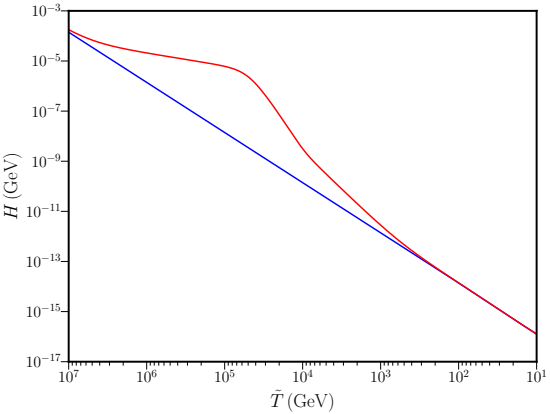

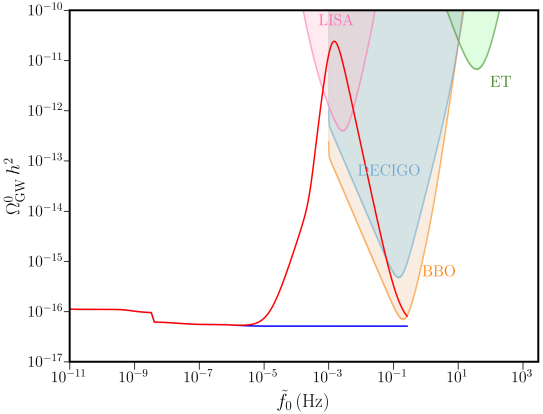

The Hubble expansion rate (on the left) and the GW spectrum (on the right) have been plotted for the purely disformal D-brane scenario. The quantities in the purely GR scenario have been plotted in blue, while the modified quantities have been plotted in red.

Shifting the peak of the GW spectrum

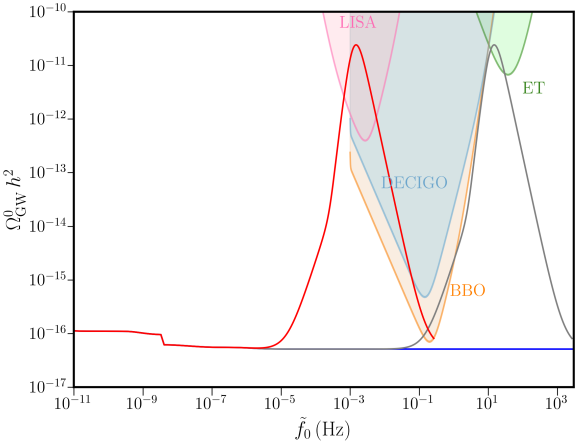

Comparison of GW spectra for the purely disformal D-brane scenario (red and grey solid lines). The GW spectra in the purely GR scenario has been plotted in blue.

Comparison of the three purely disformal cases

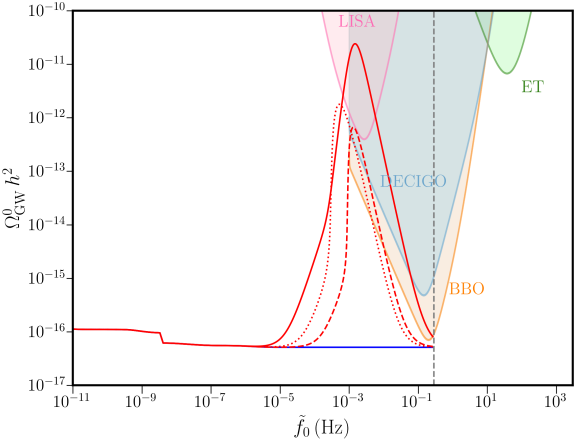

Comparison of GW spectra for the purely disformal D-brane scenario (red solid line), and the phenomenological cases with constant disformal factor (red dashed line), and field dependent disformal factor (red dotted line). The GW spectra in the purely GR scenario has been plotted in blue.

Conformal+disformal case ($C \neq 1$) with zero initial velocity

We choose

$$C(\varphi) = (1 + b\,\mathrm{e}^{-\beta\varphi})^{2n},$$

with $b = 0.1,\ \beta = 8$.

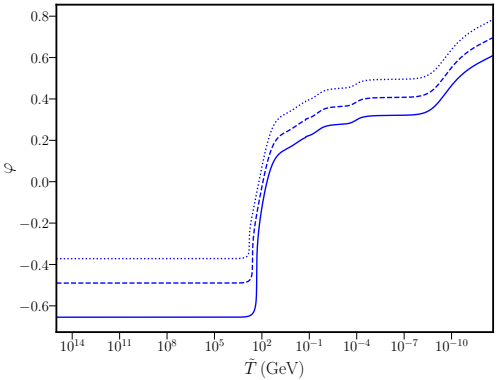

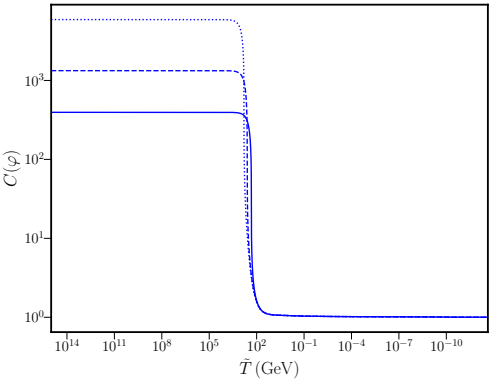

The evolution of the field and the conformal factor for $n = 1$ (solid blue line), $n = 2$ (dashed blue line), and $n = 4$ (dotted blue line).

Conformal+disformal case ($C \neq 1$) with negative initial velocity

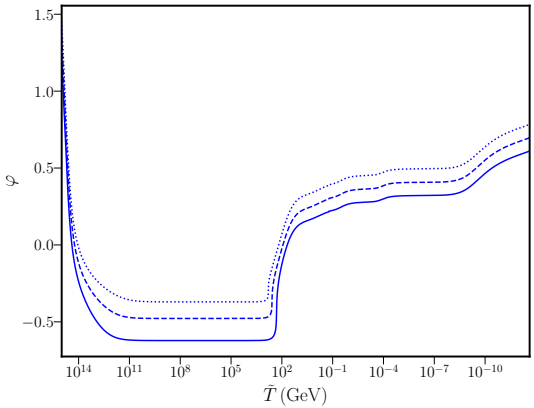

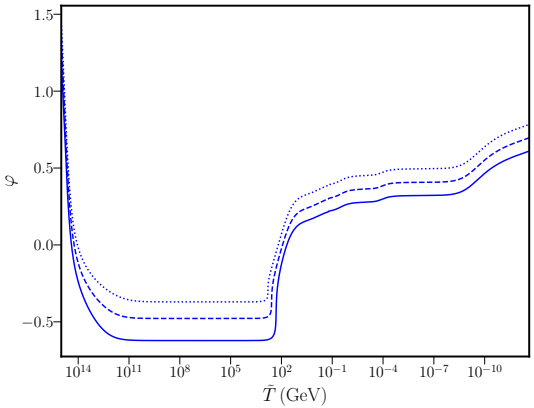

The evolution of the field and the conformal factor for $n = 1$ (solid blue line), $n = 2$ (dashed blue line), and $n = 4$ (dotted blue line), with the same conformal factor as in the previous plot.

Comparison of expansion rates

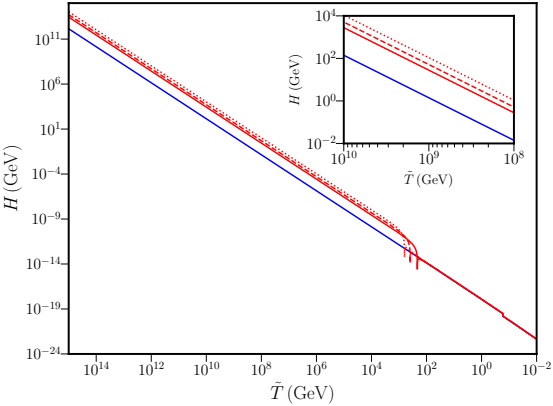

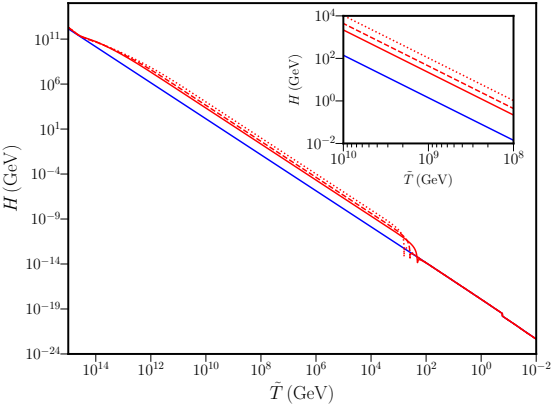

Comparison of expansion rates for the cases with zero initial velocity (on the left), and negative initial velocity (on the right). The Hubble parameter in the purely GR scenario has been plotted in blue, while the modified Hubble parameters have been plotted in red for $n = 1$ (solid red line), $n = 2$ (dashed red line), and $n = 4$ (dotted red line).

Comparison of GW spectra

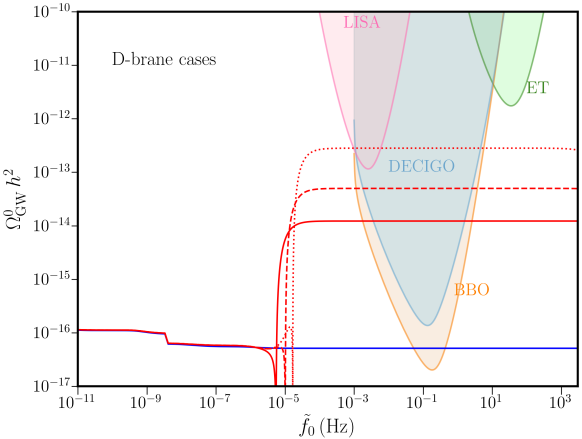

Comparison of GW spectra for the cases with $n = 1$ (solid red line), $n = 2$ (dashed red line), and $n = 4$ (dotted red line). The GW spectrum in the purely GR scenario has been plotted in blue.

Power law vs. broken power law profiles

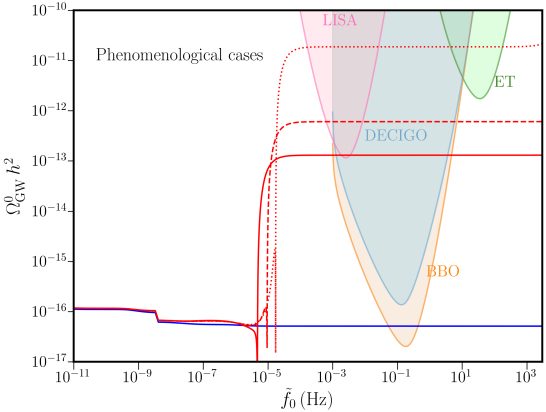

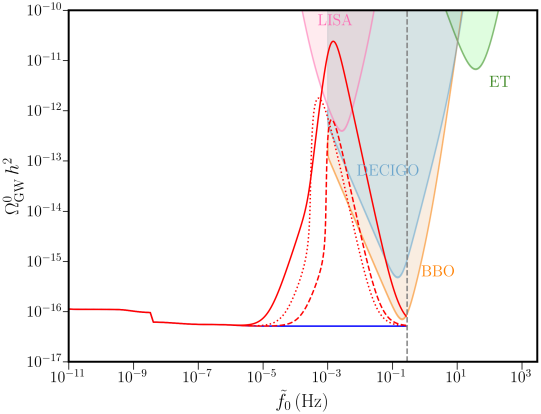

Comparison of GW spectra for purely conformal and purely disformal cases.

Power law integrated sensitivity curves

GW spectra described by the following power law form are assumed:

$$\Omega_{\rm GW}(f) = \Omega_\beta \left(\frac{f}{f_*}\right)^\beta .$$

For a set of β and some choice of f_*, the following amplitude is evaluated:

$$\Omega_\beta = \frac{\rho}{\sqrt{2T}} \left[\int_{f_{\rm min}}^{f_{\rm max}} {\rm d}f \, \frac{(f/f_*)^{2\beta}}{\Omega_{\rm eff}^2(f)}\right]^{-1/2} .$$

For each pair (β, Ω_β), $\Omega_{\rm GW}(f)$ is plotted against f.

The resulting envelope of the family of such curves is the PLS curve[5]:

$$\Omega_{\rm GW}^{\rm PLS}(f) = \max_\beta \left[\Omega_\beta \left(\frac{f}{f_*}\right)^\beta\right] .$$

[5] E. Thrane and J. D. Romano, Phys. Rev. D **88**, 124032 (2013).

Plotting the envelope

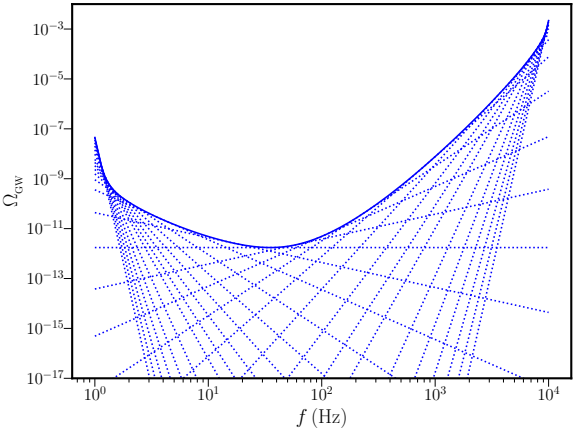

PLS sensitivity curve for Einstein Telescope.

PLS curves for different GW experiments

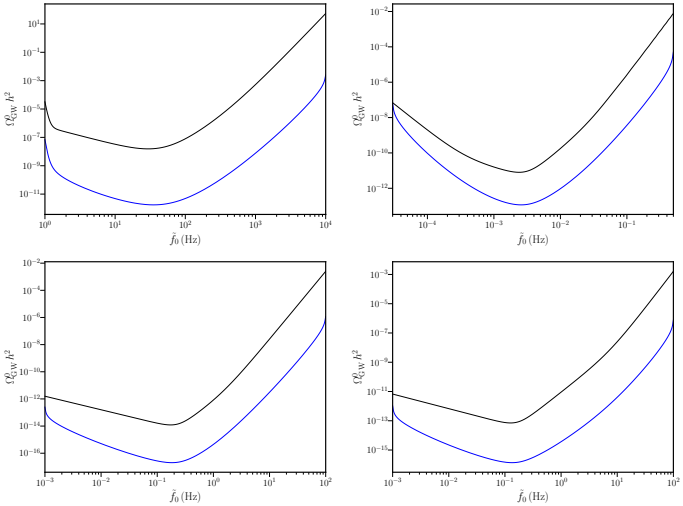

Nominal (black solid line) and PLS (blue solid line) sensitivity curves have been plotted for Einstein Telescope (upper left), LISA (upper right), BBO (lower left), and DECIGO (lower right).

Broken power law integrated sensitivity curves (BPLS)

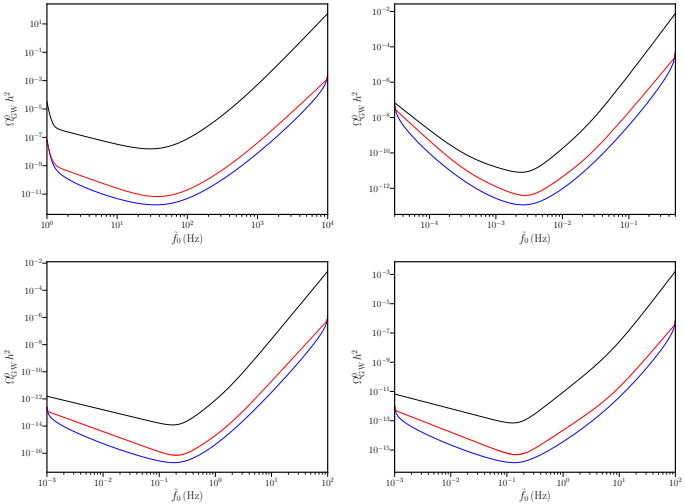

Nominal (black solid line), BPLS (red solid line), and PLS (blue solid line) sensitivity curves have been plotted for Einstein Telescope (upper left), LISA (upper right), BBO (lower left), and DECIGO (lower right).

Summary

- Modifications to the expansion rate of the early universe leave imprints on the gravitational wave spectra.
- We have studied the effects of such modifications when there are conformal and disformal couplings.
- We have found that for certain choice of initial conditions, most of such scenarios can lead to amplification of the PGW spectra.
- The modified spectra could be detected by future GW experiments.
- We have introduced the concept of broken power law sensitivity curves (BPLS) as a graphical tool to show the sensitivity of GW experiments to scenarios producing stochastic GW background (SGWB) spectra with broken power-law profiles.

Thank you!